



# UNIVERSITÀ DI PARMA

## ARCHIVIO DELLA RICERCA

University of Parma Research Repository

Inverse heat transfer modeling applied to the estimation of the apparent thermal conductivity of an intumescent fire retardant paint

This is the peer reviewed version of the following article:

*Original*

Inverse heat transfer modeling applied to the estimation of the apparent thermal conductivity of an intumescent fire retardant paint / Bozzoli, F.; Mocerino, A.; Rainieri, S.; Vocale, P.. - In: EXPERIMENTAL THERMAL AND FLUID SCIENCE. - ISSN 0894-1777. - 90:(2018), pp. 143-152. [10.1016/j.expthermflusci.2017.09.006]

*Availability:*

This version is available at: 11381/2851171 since: 2021-10-14T17:42:53Z

*Publisher:*

Elsevier Inc.

*Published*

DOI:10.1016/j.expthermflusci.2017.09.006

*Terms of use:*

Anyone can freely access the full text of works made available as "Open Access". Works made available

*Publisher copyright*

note finali coverpage

(Article begins on next page)

# Inverse heat transfer modeling applied to the estimation of the apparent thermal conductivity of an intumescent fire retardant paint

F. Bozzoli, A. Mocerino, S. Rainieri, P. Vocale  
Department of Engineering and Architecture - University of Parma  
Parco Area delle Scienze 181/A, 43124 Parma, Italy.

E-mail address of the corresponding author (Sara Rainieri): sara.rainieri@unipr.it

## Abstract

Intumescent paints are widely used as passive fire protective materials in the building sector, primarily with regard to steel framed structures. The fire resistance of commercial intumescent coatings is typically tested experimentally using expensive and time consuming large-scale tests; conversely, the increasingly common performance-based fire safety engineering approach requires the development of techniques to generalize and predict the behavior of these protective materials. Recently, an experimental and data processing technique based on temperature measurements of the growing char layer and on the formulation of the inverse heat conduction problem within the system, has been proposed. This investigation indicated that an accurate and complete modeling approach is required to make robust predictions in the processing of the experimental data. In this paper, an enhanced procedure for estimating the apparent thermal conductivity of the intumescent paint is proposed and validated. The analysis presented in this study, performed with a physical and chemical characterization of the intumescent paint, allows estimation of the apparent thermal conductivity of the char layer with good approximation, thereby providing important information for assessing the fire protective capability of the coating under the fire safety engineering approach.

Keywords: apparent thermal conductivity, parameter estimation, Inverse Heat Conduction Problems (IHCP), fire safety engineering

## 1. Introduction

In the fire safety engineering field, an increasing interest in passive fire protective materials has been observed in recent years (see [1-4]). Regarding modern building construction, which is mostly dominated by steel framed structures, the performance-based fire safety design approach is often based on the use of passive fire protective materials, either reactive or non-reactive, such as plaster or calcium silicate boards, mortars and intumescent coatings. Among these techniques, intumescent coatings are certainly the most competitive because of several advantages; assuring the desired fire resistance requirement and simultaneously be easily applied on-site to complex shapes, having an attractive surface finish, being lightweight and cost that is not excessive.

Intumescent paints, both solvent or water based [5-8], are typically applied with a thickness ranging from 1 to 8 millimeters and are designed to not burn and perform under severe conditions with the aim of maintaining a steel integrity between 1 and 3 hours in case of fire [9,10].

The fire resistance of a commercial coating is usually tested experimentally using large-scale tests. Under this approach, each commercial coating-beam configuration has to be tested one-by-one, with possible interpolation in accordance with the assessment methods. However, high operation costs, poor repeatability, unrealistic and/or inappropriate boundary conditions, and poor statistical confidence persist as common issues regarding the use of standard fire resistance tests [7].

On the other hand, performance-based structural fire engineering is increasingly common, and has become more widely accepted as a method of structural fire resistance design. According to this approach, it is important to accurately understand and predict the performance of reactive coatings [6]. Several methods for performance-based fire engineering design have been studied and applied to the fire resistance capability of structural elements protected with intumescent coatings. Most of these methods are based on numerical modeling under the assumption of equivalent thermal properties of the reactive material.

Several works have been presented on this topic in the literature [1,2,7], and most of them proposed to describe the thermal behavior of the reactive material by solving the unsteady energy balance in the system. According to this methodology, the directly measured parameters are the temperature of steel substrate and the gas temperature of the gas furnace or the heat flux released by a cone calorimeter.

Note that under this approach, either the equivalent thermal resistance [11] or the thermal conductivity are generally determined [12,13]. Regarding the thermal conductivity, either the effective value (referred to as the initial dry film thickness of the coating), or the apparent value (referred to as the expanded coating thickness) are generally considered. In most of the investigations presented in the literature, the thermal conductivity of the coating is reported as a function of temperature (see [12]). Recently, Li et al. [14] suggested the use of temperature averaged effective thermal conductivity to predict the temperature history of protected steel sections. The concept of effective thermal conductivity based on the initial dry film thickness derives from the approach adopted in Eurocode EN 1993-1-2, in which a simple equation that links this quantity to the temperature increase of steel with respect to a normalized fire curve is suggested [15].

This approach, although widely adopted in engineering design practice, provides an imprecise description of the thermal behavior of the protective layer, since it incorporates several phenomena that occur in the intumescence process into the effective thermal conductivity, which is reflected in extremely high variability of the values reported in the literature for this quantity [16].

This variability can be justified by observing that the thermal conductivity of the intumescent coating is expected to depend on the heating condition that strongly affects the intumescence process, on temperature (i.e., time) and on the initial film thickness.

Most of the experimental methodologies adopted in the above referenced papers suffer from the weakness correlated to the determination of free boundary variables of the intumescent layer or from other simplifying assumptions [17]. In particular, determining the net heat flux absorbed by the coating layer is complex, because of the uncertainty in parameters that characterize its thermal interaction with the surrounding environment, such as the coefficients of absorption, reflection and emission of the surface, the view factor towards the environment, surrounding temperature and convection coefficient. Moreover, the presence of exothermic and/or endothermic phenomena causes modeling this problem to be very complex [4].

To overcome this problem, recently Calabrese et al. [7,17] suggested an innovative experimental methodology based on the use of temperature sensors placed directly inside the expanding intumescent layer and on an approximate measurement of the net heat flux through the system. This approach, coupled with the formulation of the Inverse Heat Conduction Problem (IHCP) within the system [18-23], does not require the definition of the free boundary variables of the intumescent layer and the apparent thermal conductivity of the reactive material becomes the only parameter of the paint that has to be estimated.

In this paper, the inverse problem approach methodology is adopted and its robustness in predicting the temperature-time history of steel specimens coated with water based intumescent coatings is verified under cone calorimeter test conditions. The estimation procedure proposed in [17] is improved to better estimate the apparent thermal conductivity of the char layer of the intumescent paint. In particular, enhanced modeling of the experimental setup and thermal boundary conditions has been developed to accurately quantify the net heat flux that flows through the intumescent layer. This information enables a robust formulation of the IHCP within the system, which is based on the direct measurement of the temperature response of the layer during the intumescent phase. To validate the

proposed procedure, a numerical model is developed within the Comsol Multiphysics® 5 environment.

Moreover, the proposed procedure has been applied to the thermal characterization of two steel specimens coated with water-based intumescent coatings subject to cone calorimeter tests. Finally, the characterization of the reactive material behavior is completed with a description of the chemical and physical changes occurring during the intumescence process.

## 2. Experimental Setup

The paint adopted in this analysis is a water-based intumescent coating (PROMAPAINTE by Promat), with ingredients consisting of a PVC polymeric resin with additives such as titanium Dioxide, Melamine, 2-Butoxyethanol and others. First, a physical and chemical characterization of the intumescent paint has been performed: in particular, a Differential Scanning Calorimetric (by a PerkinElmer DSC7) and a Thermo-Gravimetric Analysis (by a Seiko Instruments Exstar 6000 TGA) have been performed to investigate the changes occurring in the physical and chemical properties of the material as a function of increasing temperature.

Further, an analysis focusing on the thermal characterization of the reactive layer has been carried out. The paint was deposited with a Dry Film Thickness (*DFT*) of 0.8 mm and 1 mm on square steel plates, 4 mm thick and 100 mm wide, as shown in Fig. 1(a). The specimens were subjected to cone calorimeter (by Fire Testing Technology Ltd.) tests under a condition characterized by a nominal radiant heat flux of 50 kW/m<sup>2</sup>.

A specimen holder made of 200 mm thick low-density calcium silicate board to minimize and control heat losses toward the environment, was used as a cradle for the specimens, as shown in Fig. 1(b). The temperature of the steel plate, foam layer and calcium silicate layer was measured using K-type thermocouples, as sketched in Fig. 1(c). The temperature in the foam layer was measured using three thermocouples, labeled  $TC_1$ ,  $TC_2$  and  $TC_3$  placed at different distances  $z_1$ ,  $z_2$  and  $z_3$  from the steel plate surface, as shown in Fig. 1(c).

These temperature sensors, shown in Fig. 1(b), were installed through 1.5 mm holes, passing through the sample holder and the coated steel specimen. This arrangement prevents the thermocouples from moving during the growth of the intumescent. The optimized horizontal distances between  $TC_1$ ,  $TC_2$  and  $TC_3$  were obtained by a numerical simulation to minimize the reciprocal influence of the thermocouples and the border effects. The temperature of the steel plate  $T_s$ , was acquired using two K-type thermocouples located on the uncoated surface of the plate, halfway between the edge and the center. Two additional thermocouples were placed at the calcium silicate-metal plate interface and between the calcium silicate and metal holder, with the aim of estimating the amount of thermal energy lost through the base of the cradle (see Fig. 1(c)).

## 3. Problem Statement

### 3.1 Model description and governing equations

The system under investigation includes the steel plate, thermal insulating calcium silicate substrate and intumescent paint that expands with time by forming the char layer. The system is subjected to the radiant heat flux generated by the cone calorimeter, while exchanging heat with the environment. To estimate the additional thermal resistance opposed by the intumescent paint, i.e., to estimate the fire protection capability of the coating, accurate knowledge of the thermal conductivity of the charred stratum is required. In the ideal situation, this important thermal property could be directly calculated by applying Fourier's law, i.e., measuring the net heat flux through the system and the temperature spatial gradient in some locations. Unfortunately, it is not possible to implement this simple approach within the system under investigation because of the following reasons:

- determining the net heat flux absorbed by the coating layer is difficult due to the uncertainty in the parameters which characterize its thermal interaction with the surrounding environment, such as the coefficients of absorption, reflection and emission of the surface, view factor towards the environment, surrounding temperature and convection coefficient;
- the local in situ measurement of the char layer temperature suffers from the disturbance caused by the sensors themselves in the sense that a non-negligible heat flux along the thermocouple probes may produce an altered temperature field, compared to the value detectable in their absence.

To overcome these problems, a strategy to correctly reconstruct the net heat flux through the system is developed and this information is adopted as a boundary condition of the IHCP in the system that includes the char layer and thermocouple probes as well, by assuming the thermal conductivity of the char layer is an unknown parameter. To correctly reconstruct the effective heat flux distribution within the char layer, it is important to consider the detailed structure of the thermocouple probe, as sketched in Fig. 2. In particular, modeling the metal sheath that protects the sensing element is important, due to its low thermal resistance.

The energy balance of the system, in which the char is considered to reach a thickness  $L$ , is then described by the following equation with reference to the domain and coordinate system schematized in Fig. 2(a)

$$\rho c_p \frac{\partial T}{\partial t} = \nabla \cdot \lambda \nabla T \quad (1)$$

where density  $\rho$ , specific heat at constant pressure  $c_p$  and thermal conductivity  $\lambda$  assume the appropriate values for each material, i.e., char layer and thermocouple probe elements.

The boundary conditions adopted to complete the equation are a Dirichlet and a Neumann boundary condition at the lower and upper boundary of the char layer, respectively, as follows:

$$T(x, y, z = 0) = T_s \quad (2)$$

$$-\lambda \left. \frac{\partial T(x, y, z, t)}{\partial z} \right|_{z=L} = q \quad (3)$$

where  $T_s$  is the temperature of the steel substrate measured and  $q$  is the net heat flux through the system. Continuity condition for the thermal field has been considered at the interface between the different materials. An adiabatic condition on all of the lateral sides of the specimens was assumed, while the initial temperature  $T_{in}$  was imposed as follows:

$$T(x, y, z, t = 0) = T_{in}. \quad (4)$$

Concerning the heat flux  $q$  transmitted through the protective layer, Calabrese et al. [17] noted that it can be estimated with good approximation when the intumescent layer has completely developed and when it assumes an approximately constant value due to the negligible heat capacity of the coating and the calcium silicate insulating layer.

However, to better estimate the heat flux, also in the transient region, the model proposed in [17] has been improved by considering the heat stored by both the steel substrate and the calcium silicate insulating layers and the heat lost through the sidewalls. In this condition, the energy balance of the steel plate is as follows:

$$q = \frac{(Q_s + Q_{c,bottom} + Q_{c,side} + Q_{l,bottom} + Q_{l,side})}{A_s} \quad (5)$$

where  $Q_s$  is the heat absorbed by the steel substrate,  $Q_{c,bottom}$  and  $Q_{c,side}$  are the heat absorbed by the calcium silicate layers (i.e., the bottom layer and the sidewalls, respectively),  $Q_{l,bottom}$  and  $Q_{l,side}$  indicate the heat lost through the bottom wall and the sidewalls, respectively, and  $A_s$  is the surface area of the steel plate (i.e.,  $A_s = l^2$ , see Figure 1 (a)).

Note that the assumption of negligible heat losses in the experiments aimed at the estimation of the equivalent thermal conductivity is a fundamental hypothesis of many researchers, i.e., in Mesquita et al. [24] and Anderson et al. [25]. Disregarding the heat losses in the energy balance equation of the steel plate (Eq. (5)) may result in an underestimation of the heat flux through the foam layer and, as a consequence, may result in an equivalent thermal conductivity value less than the actual value.

The heat absorbed by the steel and the calcium silicate layers can be evaluated by considering the density, specific heat and volume of each material and by evaluating the temperature time variation of both the steel plate and calcium silicate layers, as follows:

$$\begin{aligned} Q_s &= A_s \cdot s_s \cdot \rho_s \cdot c_s \cdot \frac{dT_s}{dt} = l^2 \cdot s_s \cdot \rho_s \cdot c_s \cdot \frac{dT_s}{dt} \\ Q_{c,bottom} &= A_{c,bottom} \cdot s_c \cdot \rho_c \cdot c_c \cdot \frac{dT_c}{dt} = l^2 \cdot s_c \cdot \rho_c \cdot c_c \cdot \frac{dT_c}{dt} \\ Q_{c,side} &= A_{c,side} \cdot s_c \cdot \rho_c \cdot c_c \cdot \frac{dT_c}{dt} = 4(l + s_c) \cdot h_c \cdot s_c \cdot \rho_c \cdot c_c \cdot \frac{dT_c}{dt} \end{aligned} \quad (6)$$

where  $\rho_s$ ,  $c_s$ ,  $s_s$  are the density, specific heat and thickness of the steel, having temperature  $T_s$ , while  $\rho_c$ ,  $c_c$ ,  $s_c$  and  $\lambda_c$  are the density, specific heat and the thickness of calcium silicate layers, having temperature  $T_c$ .

To estimate the contribution of the sidewalls, the calcium silicate layers have been considered rectangular fins; therefore, the height ( $h_c$ ) adopted in the evaluation of sidewalls surface area has been set equal to  $0.5s_c$  [26].

The heat losses through the bottom wall and the sidewalls are evaluated as follows:

$$\begin{aligned} Q_{l,bottom} &= A_{c,bottom} \cdot \frac{\lambda_c}{s_c} \cdot (T_s - T_c) = (l + 2s_c)^2 \cdot \frac{\lambda_c}{s_c} \cdot (T_s - T_c) \\ Q_{l,side} &= A_{c,side} \cdot \frac{\lambda_c}{s_c} \cdot (T_s - T_c) = 4(l + 2s_c) \cdot h_c \cdot \frac{\lambda_c}{s_c} \cdot (T_s - T_c) \end{aligned} \quad (7)$$

where  $\lambda_c$  is the thermal conductivity of the calcium silicate layers.

### 3.2 Parameter estimation procedure applied to the characterization of intumescent paint

Regarding the problem described by Eqs. (1-7), all the physical and thermal properties, except  $\lambda_a$ , are considered known quantities, while  $T_s$  and  $T_c$  (i.e., the steel and calcium silicate temperature) are measured variables. Therefore, the required information, i.e.,  $\lambda_a$ , is estimated by inversely solving Eqs. (1-7) by adopting the measured  $T_s$  and  $T_c$  time histories as input data and imposing suitable constraints. In particular, in the approach presented here, the constraints of the IHCP have been formulated by forcing, under the least square approach, the thermocouples simulated response to match the measured data values. This technique is well-known in the literature within the general approach of parameter estimation procedures [18,23]. The optimal value of the unknown parameter was then determined by minimizing the following target function under the usual least square approach:

$$F(\lambda_a) = \sqrt{\frac{1}{N} \sum_{i=1}^N \{ [TC_{1,exp} - TC_{1,sim}(\lambda_a)]^2 + [TC_{2,exp} - TC_{2,sim}(\lambda_a)]^2 + [TC_{3,exp} - TC_{3,sim}(\lambda_a)]^2 \}} \quad (8)$$

where  $N$  represents the number of time steps, subscripts *exp* and *sim* indicate the experimental and simulated temperatures of the three thermocouples  $TC_1$ ,  $TC_2$  and  $TC_3$  placed within the intumescent and  $\lambda_a$  is the apparent thermal conductivity of the char layer, which has been considered a linear function of the char layer temperature (i.e.,  $\lambda_a = \lambda_1 + a(T - T_1)$ ), with  $\lambda_1$  being the apparent thermal conductivity value of the char layer at  $T_1=500^\circ\text{C}$ .

The simulated temperature field has been determined by solving the direct problem in Eqs. (1-7) using the finite element method implemented within the Comsol Multiphysics® 5 environment. The computational mesh adopted, built with approximately 120000 tetrahedral elements and adopted to discretize the solid domain, is reported in Fig. 3. The mesh quality was verified to assure grid independent results.

The minimization of the target function (Eq. (8)) was performed through the Matlab Optimization Toolbox® using a relative tolerance on the object function less than  $1 \cdot 10^{-4}$  as a stopping criterion. The Nelder-Mead algorithm has been adopted in the minimization process.

### 3.3 Procedure validation

Validation of the procedure described in the previous sections has been performed by adopting synthetic data. A 3-D model was developed within the Comsol Multiphysics® 5 environment, considering the entire system consisting of the char layer, steel plate and calcium silicate cradle, as shown in Figure 4.

By imposing a known radiant heat flux on the upper surfaces of the model, to simulate the cone calorimeter test conditions, known values of the thermal conductivity of the char layer  $\lambda_a$ , synthetic temperature distributions of the steel substrate, calcium silicate layers and the char layer were obtained (Fig. 5).

Synthetic temperature distributions, deliberately distorted by random noise, were used as the input data of the inverse problem. In particular, white noise characterized by several values of standard deviation, specifically 0.01, 0.1 and  $1^\circ\text{C}$ , was considered.

By solving the inverse problem, i.e., forcing the temperature data corresponding to the three thermocouples  $TC_1$ ,  $TC_2$  and  $TC_3$  placed within the intumescent to match the synthetic temperature distributions (Eq. (8)), it is possible to restore the thermal conductivity of the char layer, which is the only unknown parameter.

The estimated thermal conductivity value of the char layer was then compared with the exact value used to obtain the synthetic temperature data; the comparison enables the assessment of the robustness of the modeling approach and the parameter estimation procedure.

To quantify the influence of the contributions introduced in the evaluation of the heat flux transmitted through the protective layer, the parameter estimation procedure has been performed by considering the heat flux evaluated by adopting different approaches.

The first approach considers only the contributions of heat stored in the steel and heat loss through the bottom layer of the calcium silicate, as proposed in [17]; therefore, the heat flux can be evaluated as follows:

$$q = \frac{(Q_s + Q_{l,bottom})}{A_s} \quad (9)$$

In the second approach, the contribution of the heat stored in the calcium silicate layers is considered as well:

$$q = \frac{(Q_s + Q_{l,bottom} + Q_{c,bottom} + Q_{c,side})}{A_s} \quad (10)$$

Finally, in the latter case, the heat flux transmitted through the protective layer has been evaluated by considering the full model (i.e., Eq. (5)).

The restored values of the char layer thermal conductivity were evaluated considering each of the above-discussed approaches and their relative error with respect to the reference value. They are depicted in Fig. 6 as a function of time. It is observed that heat flux estimated using Eq. (5) allows for restoring the char layer thermal conductivity with a good approximation, also in the early stage of the transient, thus verifying the robustness of the proposed approach.

On the other hand, in the steady-state regime the simplified models (i.e., Eq. (9) and Eq. (10)) are used to evaluate the heat flux with a relative error of approximately 25%. Therefore, to properly assess the heat flux  $q$  transmitted through the protective layer, all of the contributions must be considered.

Since the data presented in Fig. 6 highlight that the critical point of the procedure is related to an accurate modeling of the system and to the correct evaluation of the heat losses from the specimen, the results can be very useful to properly set-up the experimental tests (i.e., in choosing the crumble material and in positioning the thermocouples). In fact, if the thermocouples are horizontally inserted in the specimen and the material used for the crumble is characterized by low values of both thermal conductivity and specific heat, the problem can be analyzed by adopting a 1D model, thus avoiding the usage of the numerical simulation.

## 4. Results

### 4.1 Chemical and Physical characterization of the intumescent paint

The results of the Differential Scanning Calorimetric (DSC) and ThermoGravimetric Analysis (TGA) are reported in Fig. 7(a) and Fig. 7(b).

The DSC data show two endothermic phenomena (at points  $T_1$  and  $T_2$ ) that are attributed to the fusion of the polymer matrix at a temperature of approximately 186°C and the evaporation of the water chemically bound to the ingredients of the paint at a temperature of approximately 240°C, as confirmed by other authors [27]. The third phenomenon (at point  $T_3$ ) reveals an exothermic reaction due to the intumescence process activated primarily by melamine [28] that reaches its maximum at a temperature of approximately 390°C. The measured enthalpy variations for the three detected physical changes are 18.2, 28.6 and -3580 J/g, respectively. The degradation process described by the TGA curve confirms these phenomena. The intumescent process starts at a temperature of approximately 300°C, while at 400°C the char formation follows; the char degradation processes occurs above 500°C [29].

### 4.2 Thermal characterization of the intumescent paint

The experimental tests under the heat flux of a cone calorimeter was continued until the steel plate temperature reached a value of 600°C, which represents the steel critical temperature, at 6000 s (for both values of dry film thickness). Two representative images of the coated steel specimens at the end of the cone-calorimeter test are reported in Fig. 8(a) and Fig. 8(b) for  $DFT$  equal to 0.8 mm and 1 mm, respectively.

The average final thickness was approximately 37.5 mm for the specimen with  $DFT=0.8$  mm and 44.5 mm for the other specimen (i.e.,  $DFT=1$  mm). Therefore, the expansion ratio (i.e., the ratio between the final thickness and the initial thickness) is approximately 46.9 for  $DFT=0.8$  mm and 44.5 for  $DFT=1$  mm.

The time history of the steel plate,  $T_s$ , and the observed average thickness growth trend, are shown in Fig. 9(a) and Fig. 9(b) for the two  $DFT$  values considered.

The data show that the heating process of the steel substrate can be divided into three stages [17, 22]: preheating, tumescent, and post-tumescent phases. Before the substrate temperature reaches the temperature of intumescence, the heat transfer mode within the coating is dominated by conduction and the heating process is called the preheat phase. The temperatures of the virgin coating and the substrate increase quickly in this stage. When the temperature of intumescence is approached, the rise of the substrate temperature slows because of the energy consumption of the intumescent reaction. The intumescent reaction usually occurs over a temperature range, and the heating process during this stage is called the tumescent phase. At the end of the intumescent reaction, the substrate and the char temperatures rise rapidly again, and this stage is referred to as the post-tumescent phase. Thus, the temperature curve of the substrate at the tumescent phase resembles a bending curve; this type of bending evidence is a characteristic of intumescent coatings. The heating velocity decrease, even after the completion of intumescence, is due to the increased heat loss as the steel plate temperature increases significantly.

The temperature time response of thermocouples  $TC_1$ ,  $TC_2$  and  $TC_3$  is reported in Fig. 10(a) and Fig. 10(b), for the two  $DFT$  values considered in the present analysis.

The curves follow a similar pattern: a rapid increase is registered when the thermocouple is directly exposed to the heat flux emitted by the cone calorimeter apparatus. When the intumescent layer incorporates the sensors, a rapid decrease occurs while a steady state is reached late.

Minimization of the function expressed in Eq. (8) is forced by choosing several representative times in the steady state regime where the intumescent reaction has run to completion (char temperature greater than  $500^\circ\text{C}$ ), as proven by the DSC and TGA data reported in Fig. 7.

This approach (i.e., focusing on the steady state regime) enables isolating the thermal conductivity as the parameter that governs the phenomenon, while reducing the complexity of the minimization procedure as well.

The minimization has been performed by assuming the following data:  $\rho_s = 7750 \text{ kg/m}^3$ ,  $c_s = 600 \text{ J/(kg K)}$ ,  $\lambda_c = 0.1 \text{ W/(m K)}$  and a thermal conductivity equal to  $3.7 \text{ W/(m K)}$  and  $14 \text{ W/(m K)}$  for the insulation and metal sheath of the thermocouples probes, respectively.

A comparison of the experimental and restored temperatures of the three thermocouples  $TC_1$ ,  $TC_2$  and  $TC_3$  placed within the intumescent is presented in Fig. 11 for both  $DFT$  values and all time steps considered in the minimization process. The inverse procedure allows for accurate estimation of the temperatures of the three thermocouples.

To assess the robustness of the developed procedure, the temperature residuals (i.e., discrepancy between the restored values and the experimental values) were evaluated. Since the residuals are randomly distributed around zero, as shown in Fig. 12, successful implementation of the minimization procedure is confirmed.

Note that the presented results are within the range of values in the literature [29, 32-35]. For example, by investigating the behavior of intumescent paint both numerically and experimentally, Gomez-Mares et al. [29] suggested a range of thermal conductivity between 0.1 and 0.4  $\text{W/(m K)}$ , while Kandola et al. [35] obtained values within a range of 0.1 to 0.6  $\text{W/(m K)}$ .

The uncertainty of the estimated values of  $\lambda_a$  was calculated using the standard propagation error approach [30,31] as follows:

$$E_{\lambda_a} = \left\{ \sum_{i=1}^n [(\partial\lambda_a/\partial x_i) \cdot \delta_{x_i}]^2 \right\}^{\frac{1}{2}} \quad (11)$$

where the partial derivative in Eq. (11) is calculated using a finite difference approach:

$$\frac{\partial\lambda_a}{\partial x_i} = \frac{\lambda_a(x_i + \Delta x_i) - \lambda_a(x_i)}{\Delta x_i} \quad (12)$$

where  $\Delta x_i$  is a small variation of the input parameter  $x_i$ .

The values of the partial derivative for the main parameters that influence the value of apparent thermal conductivity of the char layer are presented in Table 2.

The overall percent uncertainty  $E_{\lambda a}$  was approximately 15%, assuming an uncertainty in the input parameters as reported in Table 3. For the properties of the calcium silicate, the uncertainty provided in the manufacturer's datasheet were used, while the uncertainty associated with the measurements of the temperature was estimated by monitoring the variability of the recorded quantities during the experimental tests.

## 5. Conclusions

This investigation is focused on the application of an inverse problem approach for estimating the apparent thermal conductivity of the char layer generated by intumescent paints used to protect steel framed structures in case of fire. The methodology is based on the solution of the inverse heat conduction problem within the system, under the least-square method, by adopting the measured temperature response of the char layer at different locations as known input data.

Since the solution approach requires an accurate estimate of the net heat flux through the system, the parameter estimation procedure available in the literature has been improved by developing a more accurate model.

The validation of the proposed model, performed by using synthetic data, indicates that by considering the contribution of the insulating layer in the evaluation of both heat stored and heat loss, the net heat flux through the system can be evaluated with good approximation.

Applying the validated procedure to the thermal characterization of two steel specimens coated with water-based intumescent coatings showed that the apparent thermal conductivity of the char layer moderately depends on temperature, while the initial paint thickness, for the experimental condition investigated, does not appear to have significant importance.

Moreover, the results highlight that the critical point of the procedure is related to an accurate modeling of the system and to the correct consideration of the heat losses from the specimen, therefore the here presented outcomes can be very useful to properly set-up the experimental tests.

The hereby adopted experimental data processing methodology could be considered a starting point for the definition of a reduced-scale test procedure aimed to predict the fire protective capability of intumescent paints under a performance-based fire safety engineering approach.

## 6. Acknowledgments

The authors thank the National Research Council of Italy (CNR), Trees and Timber Institute that provided the cone-calorimeter facility and the Chemistry Department of the University of Parma for the support in the DSC and TGA analysis. The authors express their sincere thanks to Dr. Marco Antonelli by Promat S.p.a. for the helpful discussion and support.

## Nomenclature

$c_p$	specific heat at constant pressure, J/(kg K)
$F$	target function, K <sup>2</sup>
$H$	height, m
$l$	length, m
$L$	final thickness of char, m
$q$	heat flux, W/m <sup>2</sup>
$s$	thickness, m
$t$	time, s
$T$	temperature, K
$x,y,z$	Cartesian coordinate, m
<i>Greek symbols</i>	
$\delta$	uncertainty

$\varepsilon_r$  relative error, %  
 $\lambda$  thermal conductivity, W/(m K)  
 $\rho$  density, kg/m<sup>3</sup>

*Subscript*

*a* apparent  
*c* calcium silicate  
*exp* experimental  
*in* initial  
*l* lost  
*s* steel  
*sim* simulated

## References

- [1] J. Alongi, Z. Hanb, S. Bourbigotc, Intumescence: Tradition versus novelty. A comprehensive review, *Progress in Polymer Science* 51 (2015) 28-73. DOI: 10.1016/j.progpolymsci.2015.04.010.
- [2] E.D. Weil, Fire-Protective and Flame-Retardant Coatings – A State-of-the-Art Review, *Journal of Fire 310 Sciences* (2011) 1-38. (DOI: 10.1177/0734904110395469)
- [3] A. Bonati, S. Rainieri, G. Bochicchio, B. Tessadri, F. Giuliani, Characterization of thermal properties and combustion behaviour of asphalt mixtures in the cone calorimeter, *Fire Safety J.* 74 (2015) 25-31. DOI: 10.1016/j.firesaf.2015.04.003
- [4] G. Landucci, F. Rossi, C. Nicoletta, S. Zanelli, Design and testing of innovative materials for passive fire protection, *Fire Safety J.* 44 (2009) 1103-1109. DOI: 10.1016/j.firesaf.2009.08.004
- [5] C. Di Blasi, C. Branca, Mathematical Model for the Nonsteady Decomposition of Intumescent Coatings, *AIChE Journal* 47 (2001) 2359-2370. DOI: 10.1002/aic.690471020
- [6] A. Elliot, A. Temple, C. Maluk, L. Bisby, Novel Testing to Study the Performance of Intumescent Coatings under Non-Standard Heating Regimes, *Fire Safety Science-Proceedings of the Eleventh International Symposium, Interscience Communications* (2014) 652-665. DOI: 10.3801/IAFSS.FSS.11-652
- [7] L. Calabrese, F. Bozzoli, G. Bochicchio, B. Tessadri, S. Rainieri, G. Pagliarini, Thermal characterization of intumescent fire retardant paints, *IOP Journal of Physics* 547 (2014) 012005. DOI: 10.1088/1742-6596/547/1/012005
- [8] Y. Zhang, Y.C. Wang, C.G. Bailey, A.P. Taylor, Global modelling of fire protection performance of intumescent coating under different cone calorimeter heating conditions, *Fire Safety J.* 50 (2012) 51-62. DOI: 10.1016/j.firesaf.2012.02.004
- [9] ISO 5660-1: 2002 Reaction to fire tests - Heat release, smoke reduction and mass loss rate - Part 1: Heat release rate (cone calorimeter method).
- [10] M. Gillet, L. Autrique, L. Perez, Mathematical model for intumescent coatings growth: application to fire retardant systems evaluation, *Journal of Physics D: Applied Physics* 40 (2007) 883-899. DOI: 10.1088/0022-3727/40/3/030
- [11] G. Li, C. Zhang, G. Lou, Y. Wang, L. Wang, Assess the Fire Resistance of Intumescent Coatings by Equivalent Constant Thermal Resistance, *Fire Technol.* 48 (2012) 529-546. DOI: 10.1007/s10694-011-0243-8
- [12] B.K. Cirpici, Y.C. Wang, B. Rogers, Assessment of the thermal conductivity of intumescent coatings in fire, *Fire Safety J.* 81 (2016) 74–84. DOI: 10.1016/j.firesaf.2016.01.011
- [13] J.E.J. Staggs, Thermal conductivity estimates of intumescent chars by direct numerical simulation, *Fire Safety J.* 45 (2010) 228-237. DOI: 10.1016/j.firesaf.2010.03.004
- [14] G. Li, J. Han, G. Lou, Y.C. Wang, Predicting intumescent coating protected steel temperature in fire using constant thermal conductivity, *Thin-Walled Structures* 98 (2016) 177–184. DOI: 10.1016/j.tws.2015.03.008

- [15] EN 1993-1-2 Eurocode 3: Design of steel structures - Part 1-2: General rules - Structural fire design.
- [16] L. Calabrese, L. Cattani, P. Vocale, Parameter Estimation Approach Applied to the Characterization of an Intumescent Fire Retardant Paints, *JP Journal of Heat and Mass Transfer* 9 (2014) 101-116.
- [17] L. Calabrese, F. Bozzoli, G. Bochicchio, B. Tessadri, P. Vocale, S. Rainieri, Parameter estimation approach to the thermal characterization of intumescent fire retardant paints, *IOP Journal of Physics* 655 (2015) 012048. DOI: 10.1088/1742-6596/655/1/012048
- [18] F. Bozzoli, G. Pagliarini, S. Rainieri, Experimental validation of the filtering technique approach applied to the restoration of the heat source field, *Exp. Therm. Fluid Sci.* 44 (2013) 858-867. DOI: 10.1016/j.expthermflusci.2012.10.002
- [19] F. Bozzoli, S. Rainieri, Comparative application of CGM and Wiener filtering techniques for the estimation of heat flux distribution, *Inverse Prob. Sci. Eng.* 19 (2011) 551-573. DOI: 10.1080/17415977.2010.531466
- [20] G.S. Dulikravich, S.R. Reddy, M.A. Pasqualetta, M.J. Colaço, H.R.B. Orlande, J. Coverston, Inverse determination of spatially varying material coefficients in solid objects, *J. Inverse Ill-Posed P.* 24 (2016) 181-194. DOI: 10.1515/jiip-2015-0057
- [21] L.A.S. Abreu, M.J. Colaço, H.R.B. Orlande, C.J.S. Alves, Thermography detection of contact failures in double layered materials using the reciprocity functional approach, *App. Therm. Eng.* 100 (2016) 1173-1178. DOI: 10.1016/j.applthermaleng.2016.02.078
- [22] C.C. Pacheco, H.R.B. Orlande, M.J. Colaço, G.S. Dulikravich, Real-time identification of a high-magnitude boundary heat flux on a plate, *Inverse Prob. Sci. Eng.* 24 (2016) 1661-1679. DOI: 10.1080/17415977.2016.1195829
- [23] J. Taler, D. Taler, Measurement of heat flux and heat transfer coefficient, in "Heat Flux. Processes, Measurement Techniques and Applications", Editors: Gianluca Cirimele, Marcello D'Elia, Nova Science Publishers, New York 2012, pp.1-103
- [24] L. Mesquita, P. Piloto, M. Vaz, Experimental study of intumescent fire protection coatings, *Fire Retardant Coatings II*, Berlin, Germany 2007
- [25] C.E. Anderson, D.K. Wauters, A Thermodynamic Heat Transfer Model for Intumescent Systems, *Int. J. Eng. Sci.* 22 (1984) 881-889. DOI: 10.1016/0020-7225(84)90036-3
- [26] T.L. Bergman, A.S. Lavine, F.P. Incropera, D.P. Dewitt, *Fundamentals of Heat and Mass Transfer*, seventh edition, JOHN WILEY & SONS
- [27] G.J. Griffin, D.A. Bicknell, J.T. Brown, Studies on the effect of atmospheric oxygen content on the thermal resistance of intumescent fire retardant coatings, *J. Fire Sci.* 23 (2005) 303-328. DOI: 10.1177/0734904105048598
- [28] J. Gu, G. Zhang, S. Dong, Q. Zhang, J. Kong, Study on preparation and fire-retardant mechanism analysis of intumescent flame-retardant coatings, *Surface e Coatings Technology* 201 (2007) 7835-7841. DOI: 10.1016/j.surfcoat.2007.03.020
- [29] M. Gomez-Mares, A. Tugnoli, G. Landucci, F. Barontini, V. Cozzani, Behavior of intumescent epoxy resins in fireproofing applications, *J. Anal. App. Pyrol.* 97 (2012) 99-108. DOI: 10.1016/j.jaap.2012.05.010
- [30] B. Blackwell, J.V. Beck, A technique for uncertainty analysis for inverse heat conduction problems, *Int. J. Heat Mass Tran.* 53 (2010) 753-759. DOI: 10.1016/j.ijheatmasstransfer.2009.10.014
- [31] J. Taler, Determination of local heat transfer coefficient from the solution of the inverse heat conduction problem, *Forschung im Ingenieurwesen/Engineering Research*, 71 (2007) 69-78. DOI: 10.1007/s10010-006-0044-2
- [32] A. Bilotta, D. de Silva, E. Nigro, Tests on intumescent paints for fire protection of existing steel structures, *Journal of Building Engineering*, 8 (2016) 198-207. DOI: 10.1016/j.job.2016.10.011

- [33] A. Bilotta, D. de Silva, E. Nigro, General approach for the assessment of the fire vulnerability of existing steel and composite steel-concrete structures, *Construction and Building Materials*, 121 (2016) 410-422. DOI: 10.1016/j.conbuildmat.2016.05.144
- [34] M. Kandula, On the effective thermal conductivity of porous packed beds with uniform spherical particles, *Journal of Porous Media* 14 (2011) 919-926. DOI: 10.1615/JPorMedia.v14.i10.70
- [35] K.B. Kandola, P. Luangtriratana, S. Duquesne and S. Bourbigot, The Effects of Thermophysical Properties and Environmental Conditions on Fire Performance of Intumescent Coatings on Glass Fibre-Reinforced Epoxy Composites, *Materials* (2015) 5216-5237. DOI: 10.3390/ma8085216

**Table 1.** Distance of the sensing element from the metal surface.

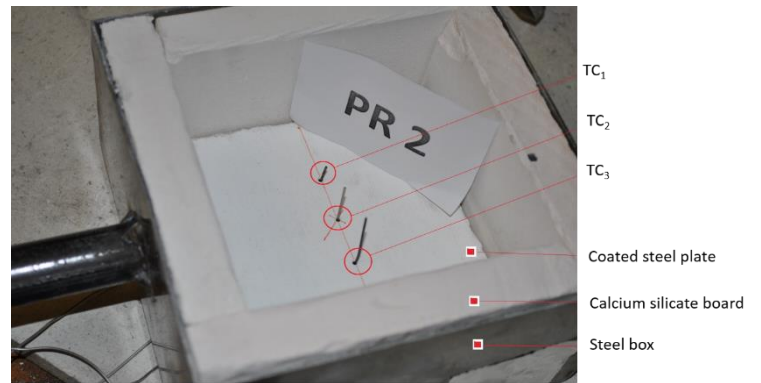
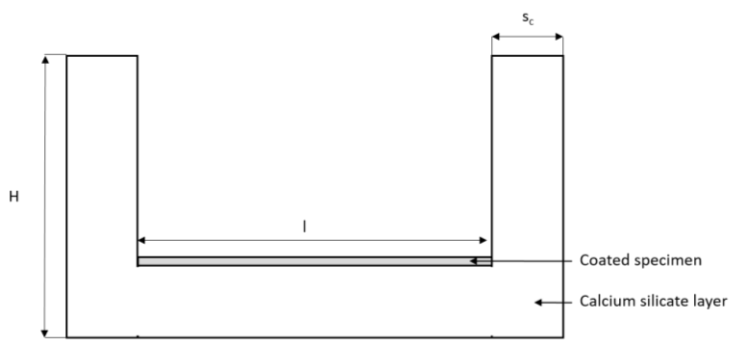
Dry film thickness (DFT) [mm]	$z_1$ [mm]	$z_2$ [mm]	$z_3$ [mm]
0.8	9.1	19.0	28.6
1.0	10.6	16.9	25.2

**Table 2.** Partial derivative for input parameters.

Parameter	$\left  \frac{\partial \lambda_a}{\partial x_i} \right $
$z$	3.47e-2 [W/(m <sup>2</sup> K)]
$T$	1.00e-2 [W/(m K <sup>2</sup> )]
$s_c$	4.00e1 [W/(m <sup>2</sup> K)]
$\rho_c$	1.02e-3 [W m <sup>2</sup> /(kg K)]
$cp_c$	4.84e-4 [kg/(s m)]
$\lambda_c$	2.30e1 [-]
$h_c$	6.00e1 [W/(m <sup>2</sup> K)]

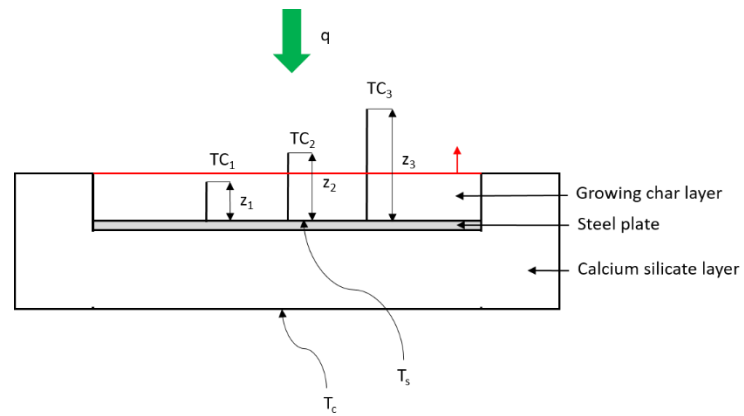
**Table 3.** Uncertainties in the model input parameters.

Parameter	$T$	$z, s_c, h_c$	$\rho_c$	$cp_c$	$\lambda_c$
Uncertainty	$\pm 5^\circ\text{C}$	$\pm 1$ mm	$\pm 5\%$	$\pm 5\%$	$\pm 10\%$



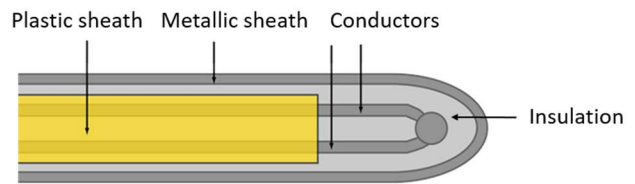
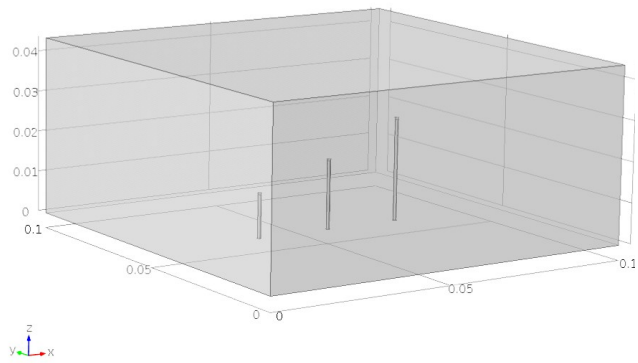
(a)

(b)



(c)

Figure 1. (a) Geometric parameters of the system under investigation. (b) Steel specimen, thermocouples and holder. (c) Details of the thermocouples location.



(a)

(b)

Fig. 2. (a) The model of the intumescent char layer instrumented with the thermocouples probes and coordinate system. (b) Sketch of the structure of the thermocouple probe.

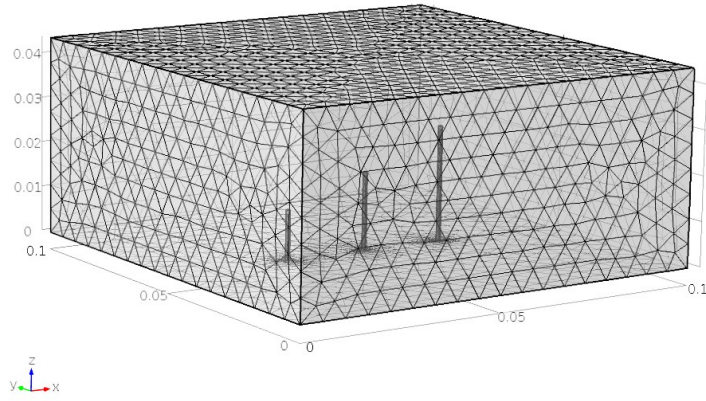


Fig. 3. The computational mesh adopted.

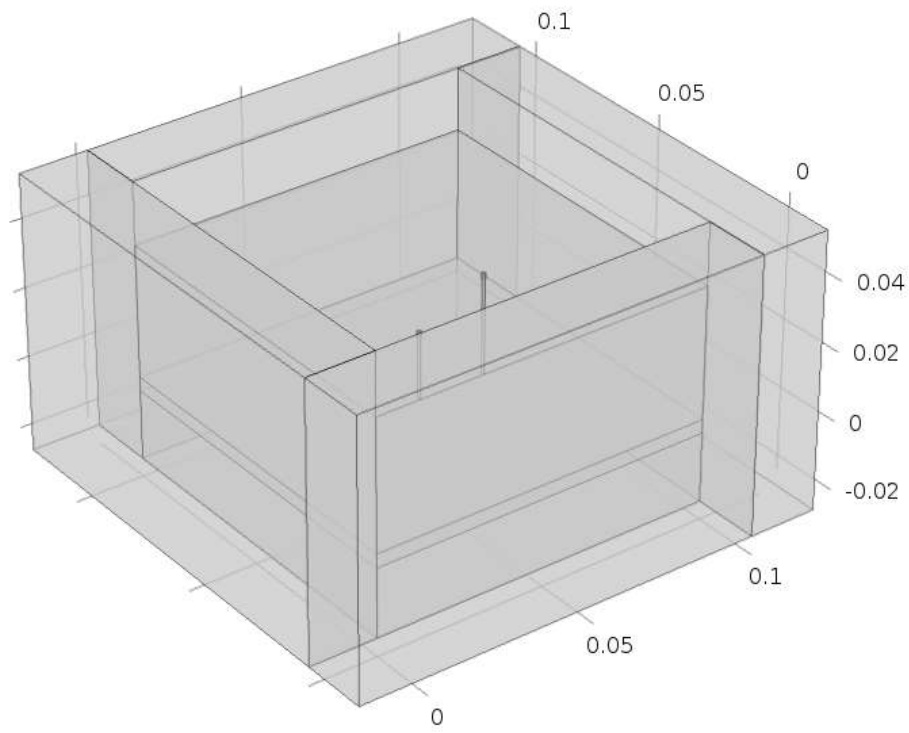
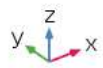


Fig. 4. 3-D model considered in the procedure validation.

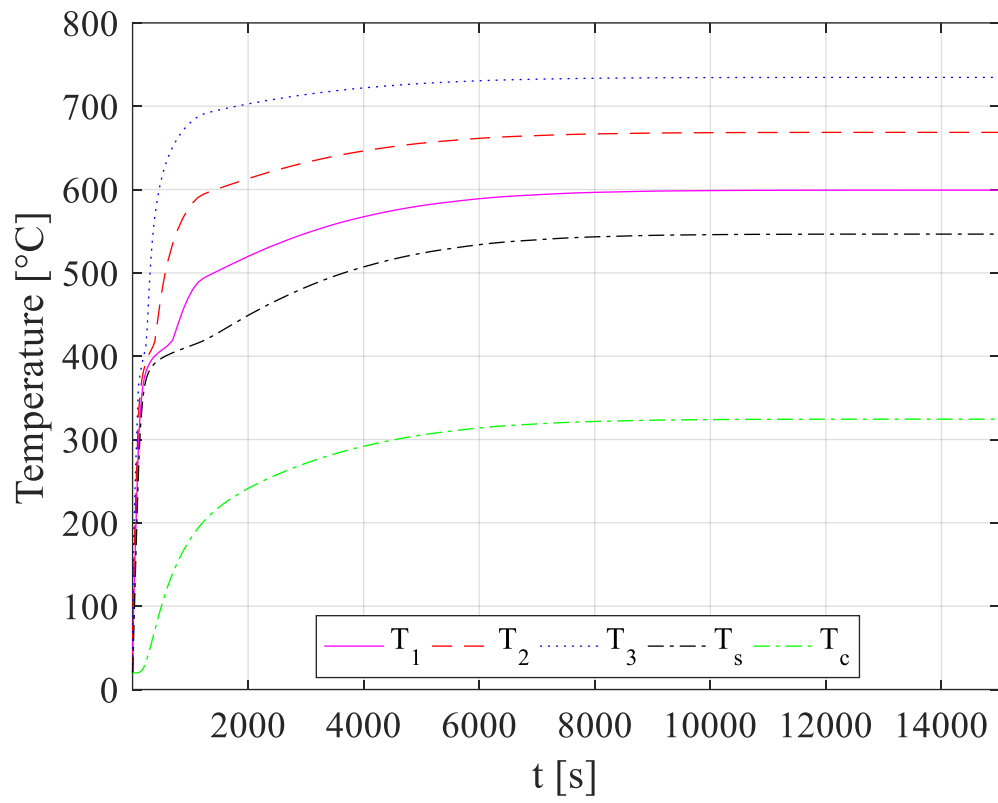
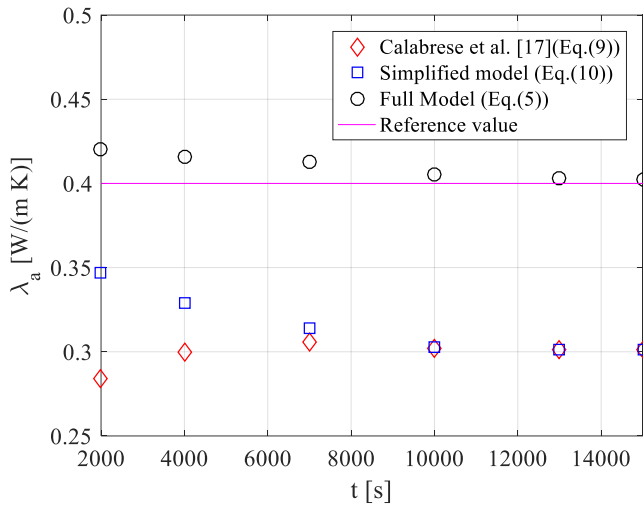
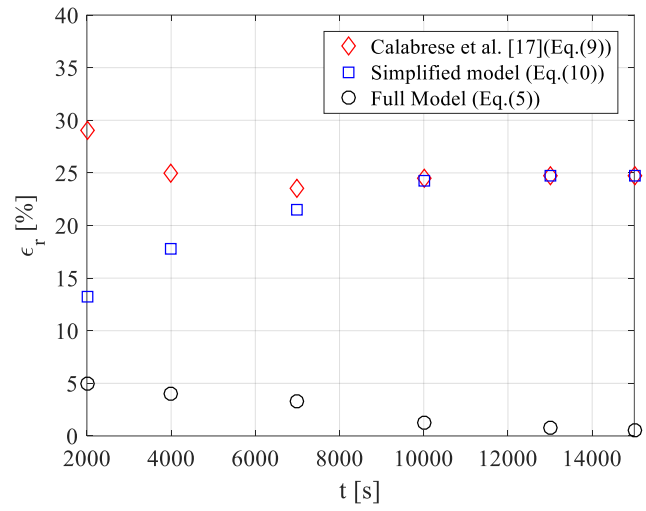


Fig. 5. Synthetic temperature distributions.

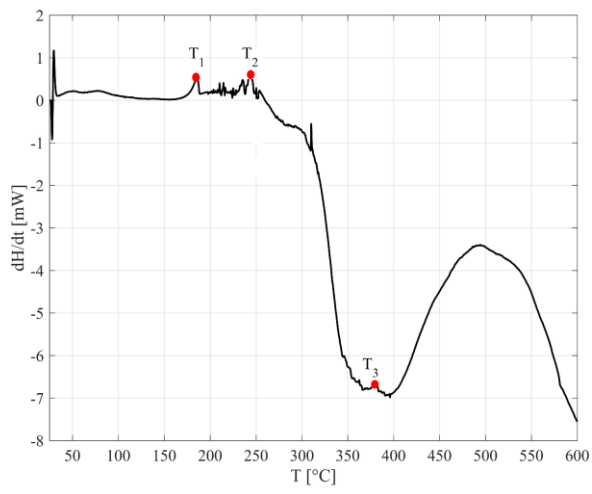


(a)

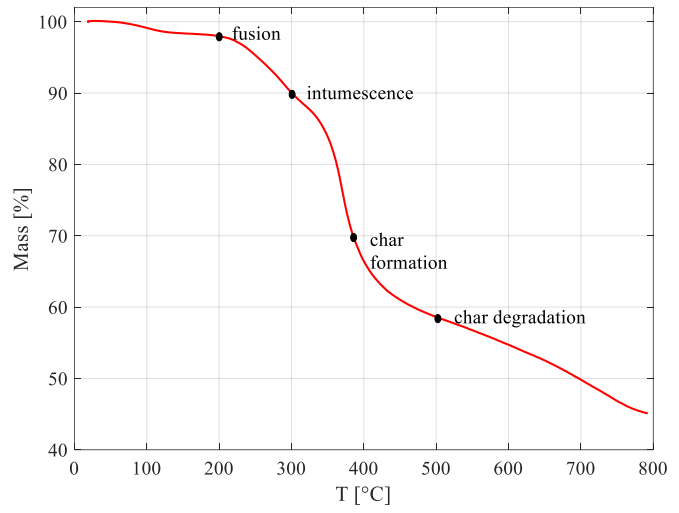


(b)

Figure 6. (a) Thermal conductivity of char layer estimated by means of different approaches. (b) Relative error on thermal conductivity of char layer.

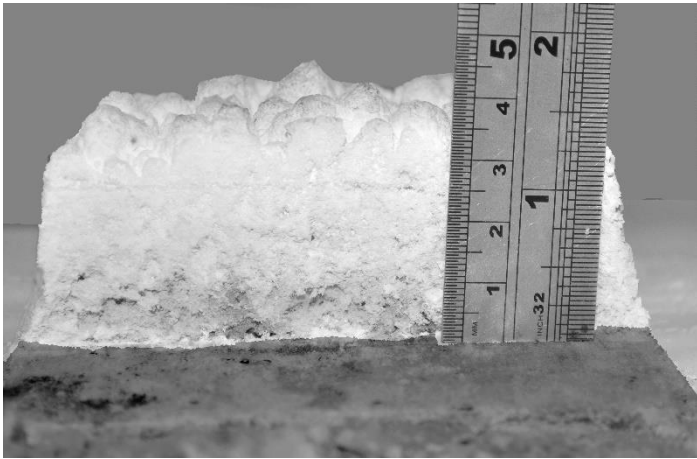


(a)

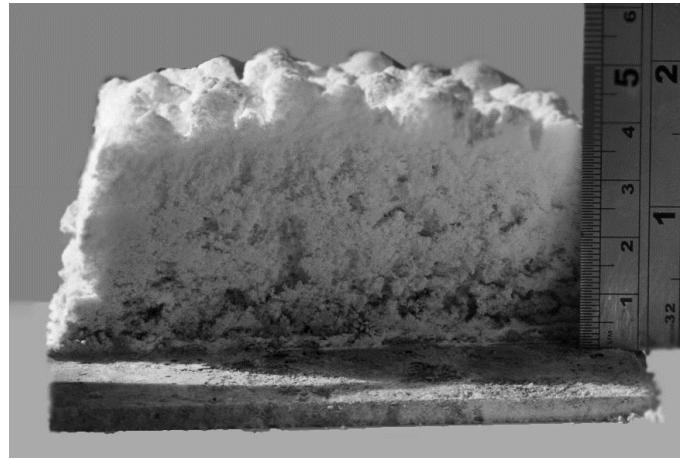


(b)

Figure 7. (a) DSC curve under a  $dT/dt = 10^\circ\text{C}/\text{min}$  condition. (b) TGA curve under a  $dT/dt = 10^\circ\text{C}/\text{min}$ .

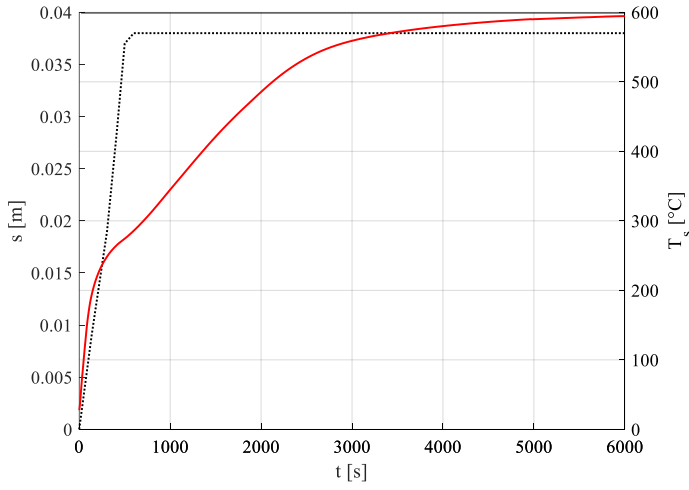


(a)

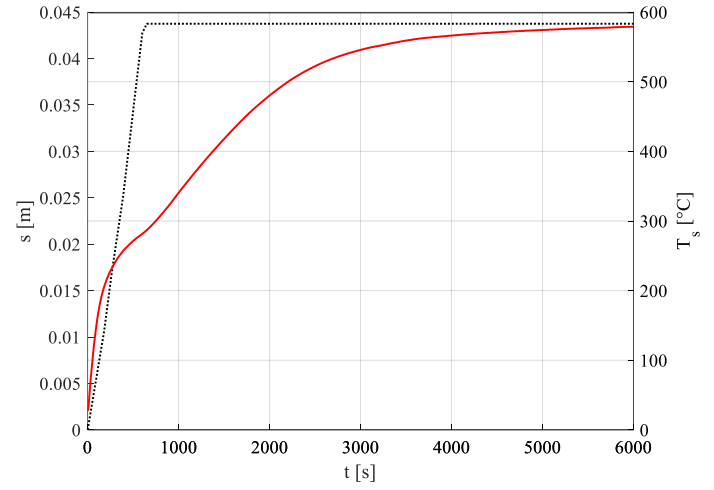


(b)

Figure 8. Representative images of the coated steel specimens at the end of the cone-calorimeter test. (a) DFT=0.8 mm (b) DFT=1 mm.

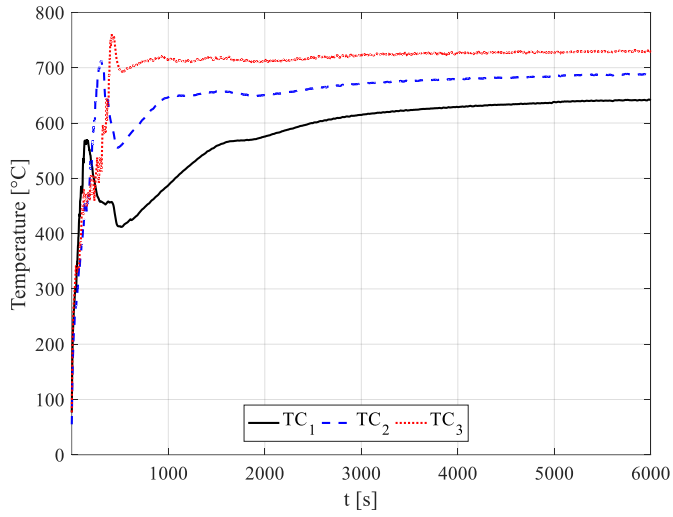


(a)

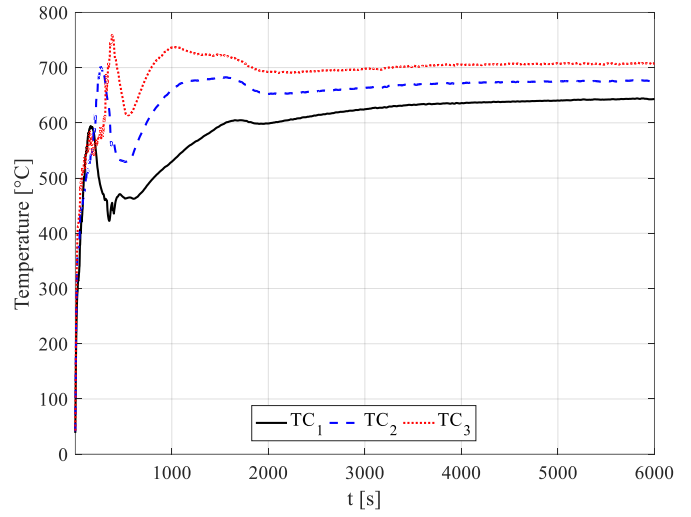


(b)

Figure 9. Steel plate temperature and char layer thickness time history. (a)  $DFT=0.8$  mm. (b)  $DFT=1.0$  mm.

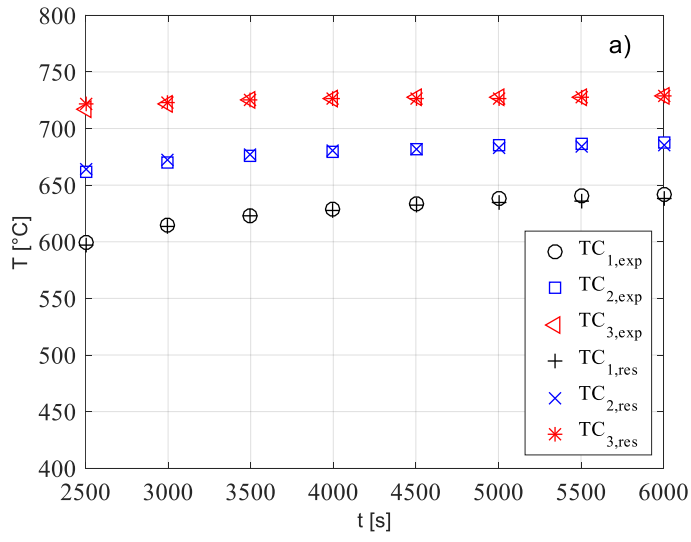


(a)

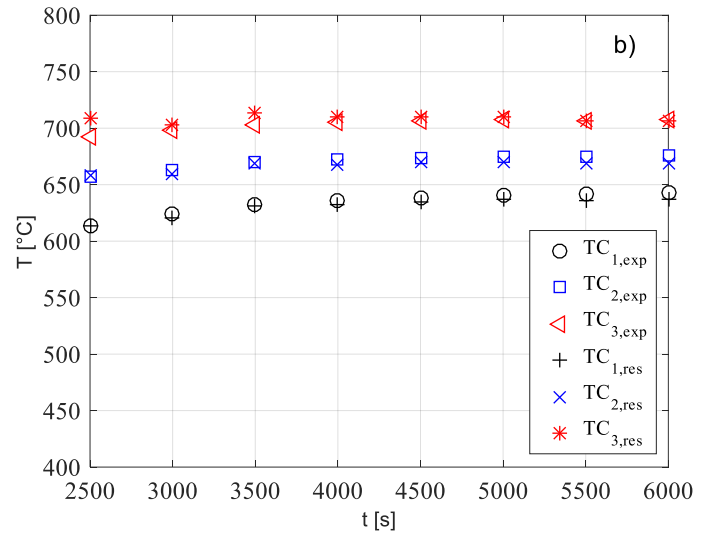


(b)

Figure 10. Temperature detected by thermocouples  $TC_1$ ,  $TC_2$  and  $TC_3$  during the intumescence process. (a)  $DFT=0.8$  mm. (b)  $DFT=1.0$  mm.

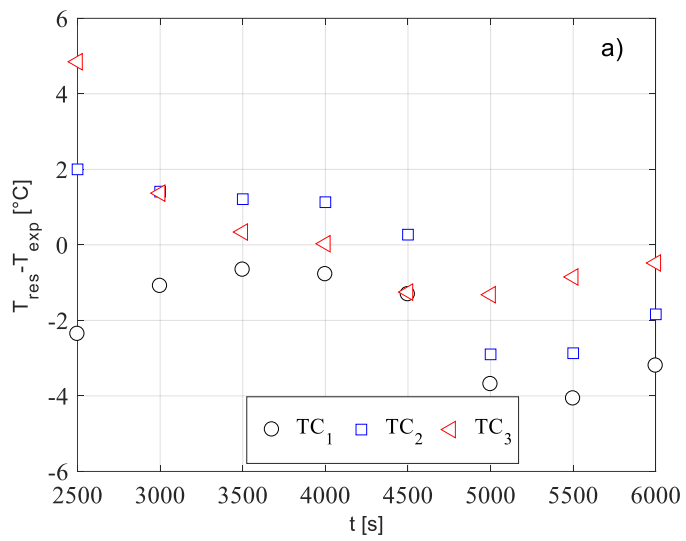


(a)

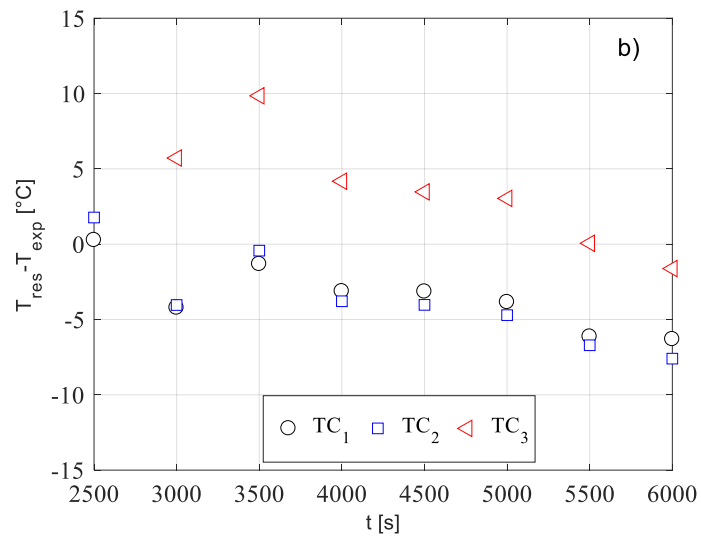


(b)

Figure 11. Comparison between the temperature detected by thermocouples  $TC_1$ ,  $TC_2$  and  $TC_3$  and the restored values. (a)  $DFT=0.8$  mm. (b)  $DFT=1.0$  mm.



(a)



(b)

Figure 12. Temperature residuals. (a)  $DFT=0.8$  mm. (b)  $DFT=1.0$  mm.